

## COMPARISON OF HIGH-PRECISION FREQUENCY-STABILITY MEASUREMENT SYSTEMS

L. Sojdr<sup>1</sup>, J. Cermak<sup>1</sup>, and G. Brida<sup>2</sup>

<sup>1</sup>Institute of Radio Engineering and Electronics, Czech Academy of Sciences, Prague, Czech Republic

<sup>2</sup>Istituto Elettrotecnico Nazionale "Galileo Ferraris", Torino, Italy

**Abstract** – The performance of two commercial high-precision frequency-stability measurement systems, Timing Solutions 5110A time-interval analyzer and Quartzlock A7 frequency and phase comparator, has been compared with two laboratory dual-mixer time-difference (DMTD) systems developed at the Institute of Radio Engineering and Electronics (IREE), Prague, and Istituto Elettrotecnico Nazionale "Galileo Ferraris" (IEN), Turin, respectively. Two BVA Oscilloquartz 5 MHz oscillators with Allan deviation (ADEV) around  $1 \times 10^{-13}$  at averaging intervals 1 s to 30 s were used as test-signal sources. In terms of the best-measurement-capability (BMC), the compared systems have shown the background noise at 5 MHz of ADEV =  $4.2 \times 10^{-14}$  at 1 s in IREE-DMTD,  $4.4 \times 10^{-14}$  in IEN-DMTD,  $7.4 \times 10^{-14}$  in A7, and  $8.8 \times 10^{-14}$  in 5110A, respectively. The 5110A analyzer behaved the best concerning the dependence on departures from the BMC conditions.

**Key words** – precision, frequency, phase, stability

main objective was to assess their performance in terms of their best measurement capability (BMC). In metrology the concept of BMC assumes the use of "near ideal" test signals which ensures that the calibration uncertainty is only due to imperfectness of the device under test. In order to approximate the BMC concept the test signals were optimized (in phase difference and power) in the cases where dependence on signal parameters had an observable impact on the results. The criterion for optimization was to minimize the system noise floor in terms of Allan deviation of fractional frequency (ADEV) at averaging interval,  $\tau$ , of 1 s. The interval of one second was chosen because of the emphasis on the short-term performance. Another goal of the comparison was assessment of the performance dependence on test-signal parameters.

In conjunction with the comparison, analysis of the RF power dependence within the dual-mixer time-difference (DMTD) structure has been made. The analysis has been applied to the DMTD structure of the IEN multiplier.

### INTRODUCTION

Comparison of high-precision frequency-stability measurement systems was carried out in the Institute of Radio Engineering and Electronics (IREE) of the Czech Academy of Sciences in the end of 2002. Laboratories that took part in the comparison were Istituto Elettrotecnico Nazionale (IEN), Italy<sup>a</sup>, Real Instituto y Observatorio de la Armada (ROA), Spain, Metrological Laboratory of the Czech Air Force (MLCAF), and IREE. Two commercial instruments were compared with two laboratory dual-mixer time-difference (DMTD) systems developed at IREE and IEN, respectively. The commercial instruments were a Timing Solution TSC5110A Time Interval Analyzer in possession of ROA and a Quartzlock A7 Frequency and Phase Comparator in possession of MLCAF. IREE, IEN and ROA took part in the comparison within the EUROMET Project No.651 on ultra-sensitive short-term frequency and stability measurement, which is coordinated by IREE.

The comparison took place in the newly established laboratory of the IREE's Department of Standard Time and Frequency<sup>b</sup>, intended specially for short-term stability measurements in time and frequency domains.

Since the compared measurement systems behave differently dependent on the parameters of the test signals, the

### SENSITIVITY-ENHANCEMENT BASICS

In high-precision frequency stability measurements, sensitivity enhancement means low-noise multiplication of the phase-time difference between two sine-wave signals. In this paragraph we will shortly mention the basics of the two sensitivity-enhancement methods employed in the systems that have been tested.

The measurement of some very stable oscillators requires measuring methods capable of resolving very small frequency fluctuations. In the time domain, counting techniques are well established [1]. It is easy to implement and it provides information on the different noise processes close to the carrier. Commercial electronic counters can resolve average fractional frequency fluctuations,  $y(\tau)$ , at best on the order of  $ADEV = 10^{-11}/\tau$ . Unfortunately this value is insufficient to characterize highly stable sources.

The resolution can be enhanced by means of the heterodyne or beat-frequency technique. Consider for example two sine-wave signals  $V_1(t) = V_{10} \sin[2\pi\nu_{01}t + \phi_1(t)]$  and  $V_2(t) = V_{20} \sin[2\pi\nu_{02}t + \phi_2(t)]$  whose frequency difference  $\nu_{01} - \nu_{02}$  is lower than their nominal frequency  $\nu_0$ . The terms  $\phi_1(t)$  and  $\phi_2(t)$  represent the random phase fluctuations of the two signals. The two signals are down-converted to a lower frequency. The beat note signal  $V_b(t) = V_0 \sin[2\pi(\nu_{01} - \nu_{02})t + \phi_1(t) - \phi_2(t)]$  retains the absolute phase fluctuations  $\Delta\phi(t) = \phi_1(t) - \phi_2(t)$ . The time fluctuations of the beat-note signal  $x_b(t) = \Delta\phi(t)/(2\pi\nu_b)$ , where  $\nu_b = |\nu_{01} - \nu_{02}|$ , can be

<sup>a</sup> Supported by ASI, the Italian Space Agency.

<sup>b</sup> Supported by Czech Grant Agency, Project #101/02/0672.

rewritten as  $x_b(t) = (v_0/v_b) \cdot x(t)$ . Thus the time fluctuations are amplified by a factor equal to the ratio between nominal frequency  $v_0$  of the oscillators and the beat-note frequency  $v_b$ . As a consequence the counter measurement uncertainty is reduced by a factor  $(v_0/v_b)$ . In the case of atomic frequency standards the beat note is inconveniently close to zero frequency. The dual-mixer time-difference technique [2, 3], shown in Fig. 1, combines the advantage of the heterodyne method with the capability to make frequency stability measurements of sources at the same frequency. It essentially consists of a pair of heterodyne systems driven in parallel with the same transfer oscillator (common oscillator) with a convenient frequency offset  $\Delta v$  with respect to the nominal frequency of the sources under measurement. Low-pass filters at the mixer outputs reject the up-conversion beat-note. The purpose of the zero-crossing detector (ZCD) is to increase the slope of the beat signal, around zero crossing, in order to reduce to a negligible level the time jitter contribution from the trigger noise of the time-interval counter (TIC).

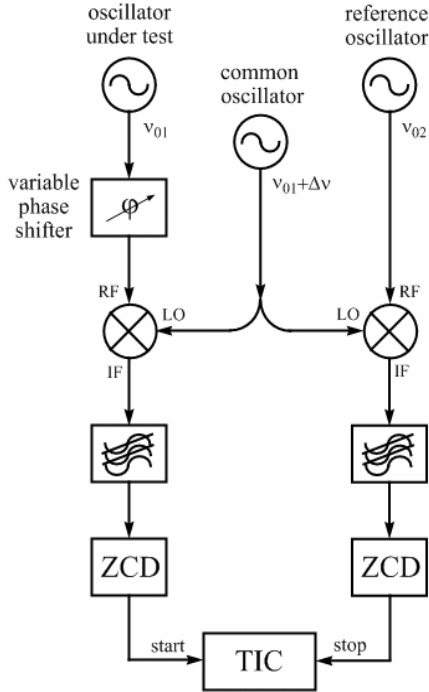


Fig. 1. Dual-mixer time-difference block diagram.

Another successful method to enhance measurement sensitivity is the frequency multiplication. The two sine-wave signals under measurement are frequency multiplied by  $m$  and then mixed and low-pass filtered. The fractional frequency fluctuation  $y_b(\tau)$  of the output beat note is  $m$  times the relative frequency departure of the input signals. This method requires two frequency multiplication chains for every different frequency of interest. The main limitation of this system is due to the additive noise of the frequency multipliers. Again the beat note frequency can be too low in

the case of frequency standards. To avoid this problem one signal is multiplied by  $m$  while the other signal is multiplied by  $(m-1)$ . The frequency of the output signals is now at the same nominal frequency  $v_0$  of the input signals. Fig. 2 depicts a block diagram for a convenient value of  $m = 10$ . This enhancement technique is known as frequency-difference multiplication [4]. Repeating this scheme by using  $N$  of these modules in cascade we achieve a multiplication factor of  $10^N$ . Because these modules operate at the same frequency extreme care must be paid to spurious coupling.

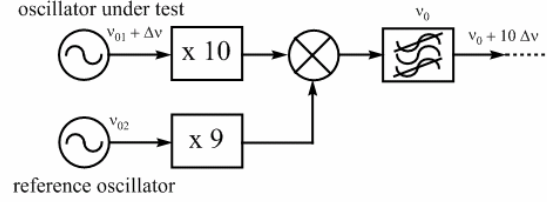


Fig. 2. Frequency difference multiplier block diagram

## DESCRIPTION OF COMPARED SYSTEMS

### A. Dual-mixer time-difference multiplier designed at IREE

The block diagram of the first version of the IREE-DMTD multiplier used in the tests is shown in Fig. 3.

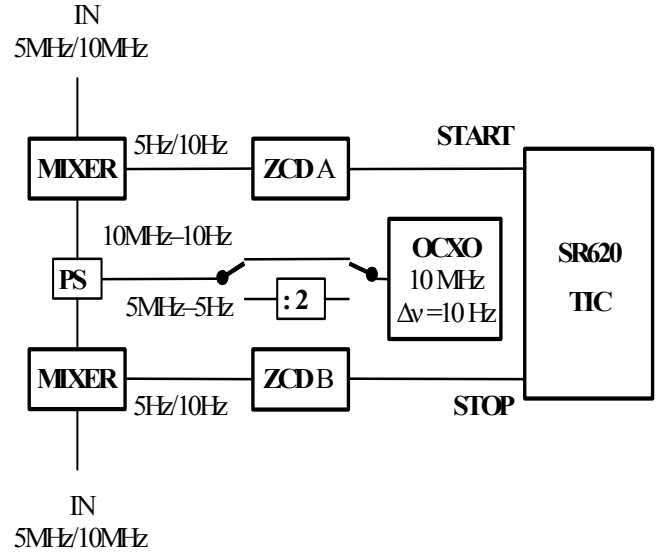


Fig. 3. Block diagram of the IREE-DMTD multiplier.

Time-difference multiplication can be made at either 5 MHz or 10 MHz. The source of the common frequency is a 10 MHz Milliren MTI 250-0502A quartz oscillator with  $ADEV = 5 \times 10^{-12}$  at 1 s offset by 10 Hz. The common sine-wave signal goes to the power splitter (PS) either directly or through a low-noise regenerative frequency divider by two. The double-balanced mixers in the version used in the comparison were Mini-Circuits RPD-1 phase detectors (in a later

modification they have been replaced with more appropriate SRA-1 mixers which have improved the multiplier noise floor by about 10 %).

The zero-crossing detector (ZCD) used in the IREE-DMTD is depicted in Fig. 4.

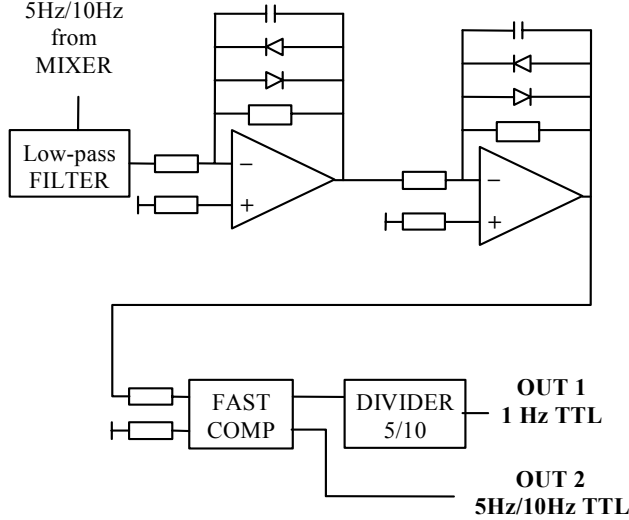


Fig. 4. Diagram of the IREE-DMTD zero-crossing detector.

The ZCD block contains two low-noise LT1028 operational amplifiers with external diode limitation. The bandwidth of each stage has been optimized to obtain the lowest noise floor [5]. The fast comparator provides TTL pulses 5Hz/10Hz that go directly to output 2 or are further divided to obtain 1 Hz. In all cases the time-difference multiplication factor is equal to  $10^6$ .

Since in this version the first-stage amplifier operates in a non-linear regime (this has been changed in the later version) the equivalent noise bandwidth cannot be calculated. We have found it experimentally by making use of the comparison with the A7 system where the bandwidth can be easily measured (see below). By injecting the same amount of additive noise in the test signals and comparing ADEV at 1 s obtained from the IREE-DMTD and A7 systems, respectively, the IREE-DMTD bandwidth was found to be about 200 Hz.

#### B. Dual-mixer time-difference multiplier designed at IEN

The laboratory dual-mixer time difference system realized at IEN follows, with minor improvements, the design architecture described in detail in [6]. The system is designed to compare high-stability frequency standards at the same nominal frequency of 5 or 10 MHz with 1 Hz beat note. As an offset oscillator in this comparison, a free-running 5 MHz Milliren MTI 260-0504A quartz oscillator with  $ADEV(1s)=7 \times 10^{-13}$  was used. The oscillator was detuned by 1 Hz. Its output power was +9 dBm. In this prototype two general-purpose ZFM-2 double balanced mixers from Mini-Circuits have been used. The zero-crossing

detectors are realized with three linear stages in cascade, each one with a bandwidth tailored to accommodate for its output-signal zero-crossing slope and to minimize additive noise contribution, followed by a fast opto-isolator used to separate ground connections, and a differential output stage. The first linear stage was designed with 10 Hz bandwidth, larger than that corresponding to the signal slope, in order to reduce the phase shifts induced by environment temperature variations. The multiplication factor for comparison at 5 MHz is equal to  $5 \times 10^6$ .

#### C. TSC 5110A time interval analyzer

The Time Interval Analyzer TSC 5110A is commercial equipment manufactured by Timing Solution for automated frequency stability measurement [7]. The instrument measures the phase difference between two input signals in the 1 MHz to 20 MHz frequency range at levels within 3 dBm to 17 dBm. It has two different modes of operation, the “single DDS mode” where the difference between two input frequencies is less than 2 Hz and the “dual DDS mode” where the input frequencies differ more than 2 Hz. We have examined the performances of this equipment in the “single DDS mode”, which is the more interesting mode for measurement of high-stability frequency standards at the same nominal frequency. In this mode the equipment operates as a dual-mixer time difference system [2, 3]. The offset generator is realized by an internal quartz oscillator and Direct Digital Synthesizer (DDS). The frequency offset is 100 Hz. The equivalent noise bandwidth is assumed to be about 450 Hz [8]. The measurement result is displayed on a screen and phase difference data are output at one second rate through a serial communication port. The TSC 5110A results reported in the next paragraph have been independently computed starting with the phase difference data collected from serial port. These results agree with the data reported on-screen by the instrument.

#### D. A7 frequency and phase comparator

The A7 Frequency and Phase Comparator is commercial equipment manufactured by Quartzlock [9] for comparison of high stability frequency standards. The system operates as a frequency-difference multiplier at 10 MHz or 5 MHz by means of an internal frequency doubler. The input signal levels must be within 6 dBm to 13 dBm range. The instrument has two modes of operation. In the so called “frequency mode” the frequency difference between the input signals is multiplied by a factor  $10^3$  at 1 MHz and 5 MHz output signals and by a factor  $10^4$  at 1 Hz output. In the “time-difference mode” the time interval between the two 1 Hz output signals corresponds to the frequency difference between inputs multiplied by a factor of  $10^4$ . We have tested this equipment in this second mode of operation.

The device manual specifies the equivalent bandwidth to be about 200 Hz. This value has been verified on the basis of the frequency-domain measurement in the frequency-mode operation at 5 MHz. In adding white-phase

noise (appropriately larger than the system noise floor) to one of the 5-MHz test signals, the cutoff frequency of approximately 100 Hz was found from the frequency-domain response.

## MEASUREMENT SETUP

### A. Measurement conditions

The laboratory where comparison measurements were carried out is located under ground in the best-suited place within the IREE main building as for the electromagnetic perturbations and vibrations. The room is electrically shielded and temperature controlled to within 2° C with no abrupt variations. No other activities were being carried out in the laboratory during the comparison measurements. The picture shown in Fig.5 illustrates the measurement conditions in the laboratory.



Fig. 5. IREE laboratory for short-term frequency-stability measurement.

### B. Test signals

The test signals were generated from either of the two BVA 5MHz Oscilloquartz 8600-BC5GE ultra-stable quartz oscillators in possession of IREE. In the following text we will denote these oscillators as OQ291 and OQ315, respectively, according to their serial numbers. Each oscillator provides two output signals and allows control of its frequency by an external voltage. The frequency of OQ291 can be offset within  $-1.4 \times 10^{-7}$  (0 V) to  $+1.2 \times 10^{-7}$  (+10 V) and the frequency of OQ315 within  $-1.7 \times 10^{-7}$  (0 V) to  $+1.8 \times 10^{-7}$ . The signal power available at the outputs is as follows: 6.8 dBm at the SN291/1 output, 7.0 dBm at SN291/2, 7.1 dBm at SN315/2, and 7.2 dBm at SN315/2, respectively. During the comparison also available was a signal from a HP8662A frequency synthesizer locked to one of the BVA oscillators.

The frequency stability of the test sources specified by the manufacturer in terms of ADEV( $\tau$ ) is shown in Fig. 6. So far we have no verified uncertainties of the values presented in Fig.6.

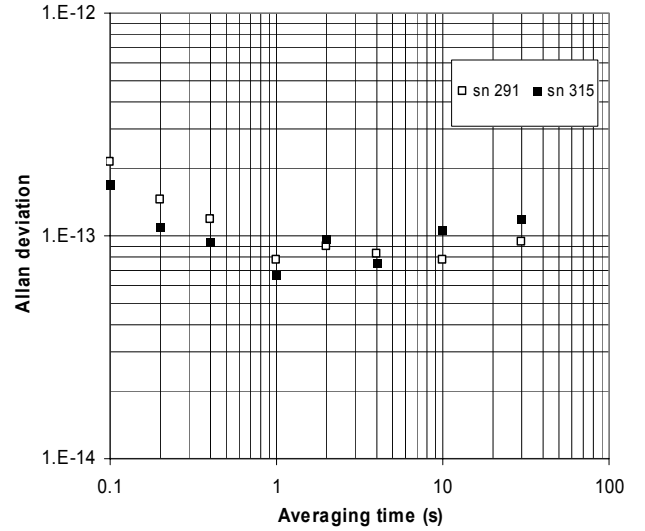


Fig. 6. Frequency stability of the test signals.

### C. Setup description

The 5110A, IREE-DMTD and IEN-DMTD units were placed in the same rack (the third one from right in Fig. 5) while the A7 unit was installed, because its dimensions did not fit with the rack, on a small metallic table nearby.

The test-signal sources were mounted close together at an adjacent rack (the next to left in Fig. 5). The same 1.2-m long cables with SMA connectors at both ends were employed for the test signals in all measurements. Connector adaptors SMA-BNC had to be used at the A7 and IREE-DMTD inputs, and SMA-BNC-TNC at the 5110A input, respectively.

A Stanford Research SR620 counter was used to measure the time interval with the IREE-DMTD, IEN-DMTD and A7 systems. The DC voltages for IREE-DMTD and IEN-DMTD were supplied from commercial linear DC sources. Phase adjustments were performed with the aid of a Femtosecond Systems FSS11A delay line or, alternatively, laboratory-made delay line based on insertion of coaxial cables of variable length. Also available was a Femtosecond Systems FSSM100 noise source capable of adding well-defined broad-band white noise into either of the 5 MHz test signals.

For the verification of the results in the frequency domain, the Femtosecond Systems phase-noise measurement suite was employed, with the noise floor specified as  $L(f) = -145 \text{ dBc/Hz}$  at  $f = 1 \text{ Hz}$  from the 5 MHz carrier, and  $L(f) = -177 \text{ dBc/Hz}$  at  $f = 100 \text{ kHz}$  from the carrier for the input level of +12 dBm.

In the case of the IREE-DMTD, IEN-DMTD and A7 systems the one-second time-difference output data were downloaded to a PC from the SR620 counter. In the case of the 5110A analyzer, the output data were downloaded directly from the device. In all cases the RS-232 links were used.

## MEASUREMENT RESULTS

### A. Optimized test signals

As mentioned above we define the optimized test signals as the ones that ensure the minimum noise-floor in terms of  $\text{ADEV}(\tau=1\text{s})$ . Given the limited time for the comparison, the “optimized” conditions have been approximated in evaluation by choosing the results with the minimum value of  $\text{ADEV}(\tau=1\text{s})$  out of all measurements performed under different conditions.

Stability analysis has been made with the assistance of Riley’s software [10]. The noise-floor plots that are characterized by the minimum value of  $\text{ADEV}$  at  $\tau=1\text{s}$  are shown in Fig. 6,7,8, and 9, respectively. The confidence bars in the  $\text{ADEV}(\tau)$  plots are the 68 % uncertainties. The dashed lines correspond to white/flicker phase-noise slopes. All the results have been obtained from instantaneous time differences (i.e. no averaging has been made). These are denoted by  $\Delta t$  while the phase-time differences between the RF signals at inputs A and B are denoted as  $\Delta x$  (for the IREE/IEN-DMTD systems  $\Delta t = m \Delta x$  holds, where  $m$  is the multiplication factor).

IREE-DMTD (Fig. 7): Test signals from OQ291/2 through power splitter; +4 dBm power at device inputs;  $\Delta x = 0.3 \text{ ns}$ ; common oscillator tuned to be coherent with the test-signal frequency as close as possible.

The departures from the  $1/\tau$  slope are due to cross-talks between the common oscillator and the test-signals.

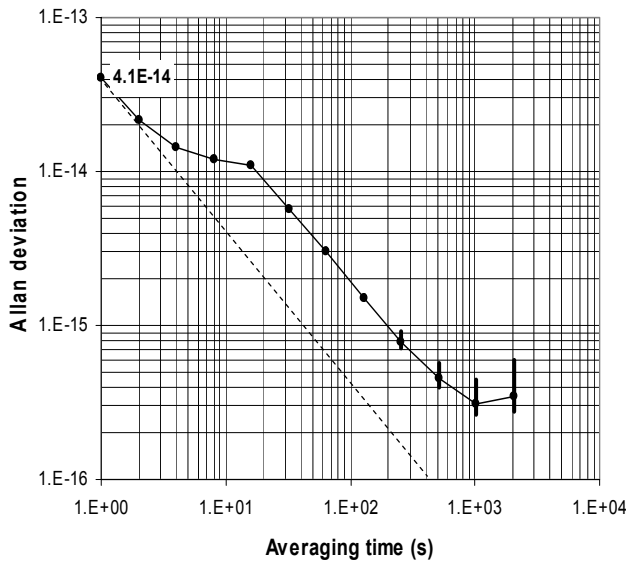


Fig. 7. Noise floor of IREE-DMTD.

IEN-DMTD (Fig. 8): Test signals from OQ291/2 to A and OQ291/1 to B; +7 dBm power at device inputs;  $\Delta x = 0.6 \text{ ns}$ .

The long-term irregularities in the Allan deviation plot are likely due to environmental temperature fluctuations and poor thermal isolation of the system at the comparison time.

Successive investigation on this aspect has shown large mixer temperature sensitivity.

The short-term effect may be caused, as in the IREE-DMTD system, by an imperfect isolation between the test signal and the common oscillator.

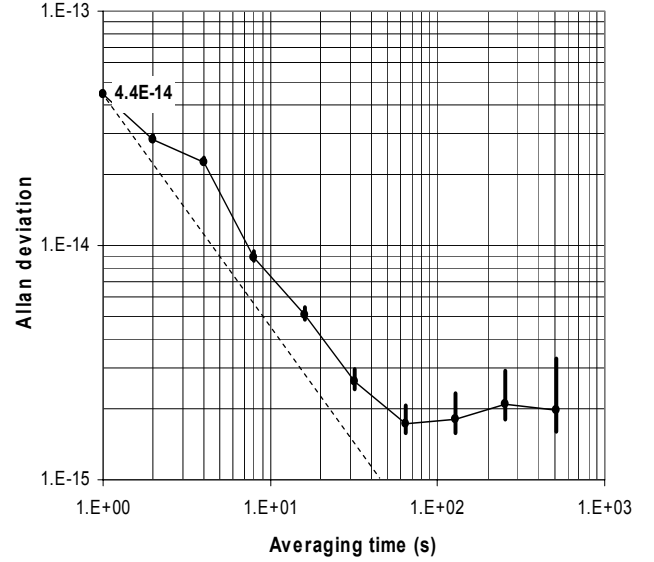


Fig. 8. Noise floor of IEN-DMTD.

A7 (Fig. 9): Test signals from OQ291/2 through power splitter; +4 dBm power at device inputs (lower than specification range).

Note: In short-term measurements of the dependence of  $\text{ADEV}(\tau=1\text{s})$  on  $\Delta x$ , a better value of  $7.4 \times 10^{-14}$  has been found (see the following paragraph).

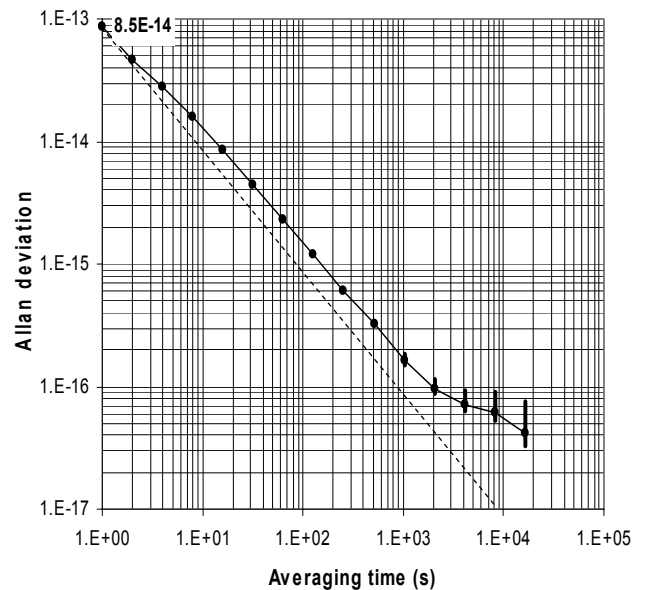


Fig. 9. Noise floor of A7.



5110A (Fig. 10): Test signals from OQ315/1 to A and OQ315/2 to B ; +7 dBm power at device inputs;  $\Delta x = 0.5$  ns.

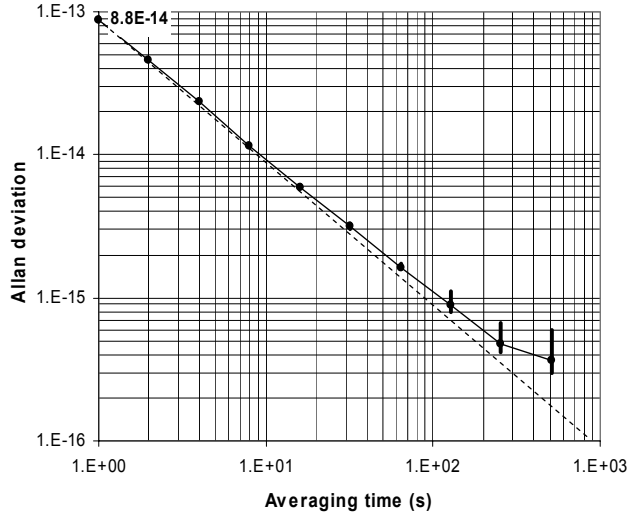


Fig.10. Noise floor of 5110A.

The above results are summarized in a graphics with the same scaling in Fig. 11.

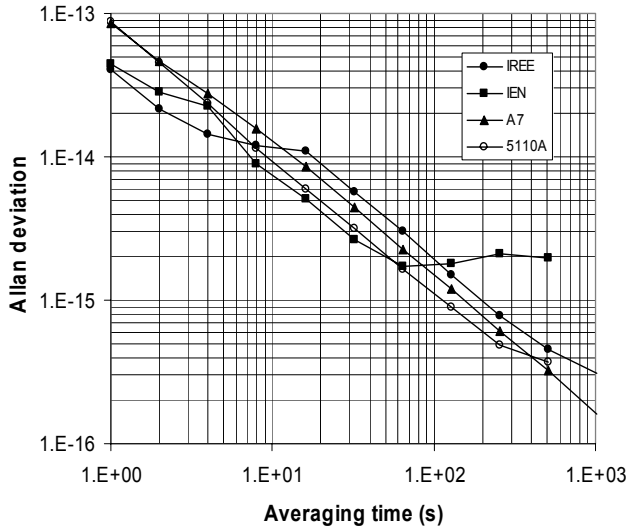


Fig. 11. Summarized comparison of the noise floor.

### B. Dependence on phase-time difference

Dependence of  $ADEV(\tau=1s)$  on input phase difference,  $\Delta x$ , has been inspected in all devices. The test signals were taken from the same source. Large phase delays ( $\Delta x > 1$  ns) were inserted through a delay line. The results are shown in the following tables together with 95% uncertainties.

IREE-DMTD (Table I): Test signals from OQ315/1 to input A and OQ315/2 to input B; delays inserted in branch B via a laboratory delay line; +4 dBm input power.

TABLE I  
DEPENDENCE OF THE NOISE FLOOR ON INPUT PHASE DIFFERENCE IN IREE-DMTD

Input phase difference (ns)	Allan deviation at $\tau=1s$	Uncertainty
0.1	$4.2 \times 10^{-14}$	$0.2 \times 10^{-14}$
0.4	$4.7 \times 10^{-14}$	$0.4 \times 10^{-14}$
0.9	$5.6 \times 10^{-14}$	$0.4 \times 10^{-14}$
10	$3.6 \times 10^{-13}$	$0.4 \times 10^{-13}$
50	$3.4 \times 10^{-13}$	$0.4 \times 10^{-13}$
95	$4.4 \times 10^{-13}$	$0.6 \times 10^{-13}$

IEN-DMTD (Table II): Test signals from OQ315/1 to input A and OQ315/2 to input B; large delays inserted into input B via the FSS11A delay line; +7 dBm input power.

TABLE II  
DEPENDENCE OF THE NOISE FLOOR ON INPUT PHASE DIFFERENCE IN IEN-DMTD

Input phase difference (ns)	Allan deviation at $\tau=1s$	Uncertainty
0.6	$4.7 \times 10^{-14}$	$0.2 \times 10^{-14}$
14	$1.7 \times 10^{-13}$	$0.2 \times 10^{-13}$
48	$3.5 \times 10^{-13}$	$0.4 \times 10^{-13}$
98	$6.4 \times 10^{-13}$	$0.6 \times 10^{-13}$

A7 (Table III): Test signals from OQ291/1 to input A and OQ291/2 to input B; large delays inserted into input B through FSS11A; the opposite large delays obtained by inverting the input signals; +4 dBm input power.

Note: The value of  $5.5 \times 10^{-13}$  found at  $\Delta x = -87$  ns is unexpected and unexplained (one would expect about the same value as at  $\Delta x = +87$  ns).

TABLE III  
DEPENDENCE OF THE NOISE FLOOR ON INPUT PHASE DIFFERENCE IN A7

Input phase difference (ns)	Allan deviation at $\tau=1s$	Uncertainty
-87	$5.5 \times 10^{-13}$	$0.6 \times 10^{-13}$
-12	$3.8 \times 10^{-13}$	$0.6 \times 10^{-13}$
-0.6	$7.4 \times 10^{-14}$	$0.4 \times 10^{-14}$
+0.6	$1.6 \times 10^{-13}$	$0.2 \times 10^{-13}$
+12	$3.4 \times 10^{-13}$	$0.4 \times 10^{-13}$
+87	$3.2 \times 10^{-13}$	$0.4 \times 10^{-13}$

5110A (Table IV): Test signals from OQ315/1 to input A and OQ315/2 to input B; large delays inserted into input B through FSS11A; +7 dBm input power.

TABLE IV  
DEPENDENCE OF THE NOISE FLOOR ON INPUT PHASE DIFFERENCE IN 5110A

Input phase difference (ns)	Allan deviation at $\tau=1s$	Uncertainty
0.6	$8.9 \times 10^{-14}$	$0.8 \times 10^{-14}$
3	$8.8 \times 10^{-14}$	$0.8 \times 10^{-14}$
14	$1.1 \times 10^{-13}$	$0.1 \times 10^{-13}$
21	$1.4 \times 10^{-13}$	$0.1 \times 10^{-13}$
48	$1.3 \times 10^{-13}$	$0.1 \times 10^{-13}$
98	$1.3 \times 10^{-13}$	$0.1 \times 10^{-13}$

### C. Dependence on input power

Care must be taken when evaluating the dependence of the noise floor on input power since it can be masked by the dependence on phase difference. This applies particularly to the A7 system where the value of  $\Delta x$  has shown very critical. Thus  $\Delta x$  should be checked and, if needed, adjusted when measuring the power dependence. In the IREE-DMTD and IEN-DMTD systems where  $\Delta t = m \Delta x$  holds it can be easily checked through  $\Delta t$  while in the two commercial systems  $\Delta x$  has to be measured directly.

The IEN-DMTD system was checked by using the test signals from a HP8662A frequency synthesizer phase-locked to OQ291 (the signal went through a power splitter to inputs A and B, respectively). The input phase difference was around 0.7 ns, i.e. within the optimum interval. The dependence on input power is shown in Table V. Notice that due to noisier test signals the minimum value of  $8 \times 10^{-14}$  is higher than the noise floor of  $4.4 \times 10^{-14}$  mentioned previously.

TABLE V  
DEPENDENCE ON INPUT POWER IN IEN-DMTD

Input power (dBm)	Allan deviation $\tau=1s$	Uncertainty
0	$1.2 \times 10^{-13}$	$0.2 \times 10^{-13}$
3	$9.3 \times 10^{-14}$	$1.0 \times 10^{-14}$
6	$8.3 \times 10^{-14}$	$0.8 \times 10^{-14}$
7	$8.0 \times 10^{-14}$	$0.8 \times 10^{-14}$
10	$8.8 \times 10^{-14}$	$0.8 \times 10^{-14}$
11	$8.9 \times 10^{-14}$	$0.6 \times 10^{-14}$

The IREE-DMTD system has not been assessed because of the disturbing effect that was assumed to impact the actual power dependence. Namely, by increasing the power from +4 dBm to +7 dBm (while keeping optimum  $\Delta x$ ) the noise floor increased from  $4.1 \times 10^{-14}$  to  $5.2 \times 10^{-14}$ , respectively. This unexpected result was suspected to be due to the mismatch of the phase detectors used inappropriately in this version (it has been proved in a later version with mixers instead of the phase detectors).

The 5110A unit was tested by inserting 3-dB attenuators in the signal paths. The test signals were taken from OQ291/1 to input A and OQ291/2 to input B. No track of  $\Delta x$  was kept during this measurement. The dependence on input power can be seen in Table VI.

TABLE VI  
DEPENDENCE ON INPUT POWER IN 5110A

Power at input A (dBm)	Power at input B (dBm)	Allan deviation $\tau=1s$	Uncertainty
7	7	$8.9 \times 10^{-14}$	$0.8 \times 10^{-14}$
4	4	$1.1 \times 10^{-13}$	$0.2 \times 10^{-13}$
7	4	$9.3 \times 10^{-14}$	$0.8 \times 10^{-14}$

The results obtained with the A7 system indicate that the strong dependence on  $\Delta x$  masks the dependence on input power in the measurements where no appropriate adjustment of  $\Delta x$  was made. Therefore these results are not presented in this text. The fact remains, however, that the minimum

noise floor in A7 reported previously has been obtained with only +4 dBm of signal power.

### D. Uncorrelated test signals

The OQ291 and OQ315 oscillators were employed as sources of uncorrelated test signals. According to specification in Fig. 6,  $ADEV(\tau)$  of both oscillators is approximately  $1 \times 10^{-13}$  in an interval of  $1 s < \tau < 30 s$ . The almost constant value of  $ADEV(\tau)$  indicates prevailing flicker frequency noise. Since in all tested measurement systems the noise floor shows  $ADEV(\tau=1s) < 1 \times 10^{-13}$  and  $ADEV(\tau)$  decreases as  $\tau$ , the noise contribution of the measurement systems can be neglected in all cases for  $\tau \gg 1 s$ . Thus for larger averaging intervals it is not the measurement systems but the test signals that are "tested". At intervals around 1 s, however, one has to discern the noise contributions from the test signals and the measurement system.

The combined frequency stability between the test signals from the OQ291 and OQ315 oscillators found with the four measurement systems can be seen in Table VII.

TABLE VII  
COMBINED ADEV BETWEEN OQ291 AND OQ315 OSCILLATORS

$\tau$ (s)	IREE ADEV	IREE Uncertainty	IEN ADEV	IEN Uncertainty
1	$1.4 \times 10^{-13}$	$0.1 \times 10^{-13}$	$1.3 \times 10^{-13}$	$0.1 \times 10^{-13}$
2	$1.4 \times 10^{-13}$	$0.1 \times 10^{-13}$	$1.3 \times 10^{-13}$	$0.1 \times 10^{-13}$
4	$1.4 \times 10^{-13}$	$0.2 \times 10^{-13}$	$1.4 \times 10^{-13}$	$0.2 \times 10^{-13}$
8	$1.6 \times 10^{-13}$	$0.3 \times 10^{-13}$	$1.5 \times 10^{-13}$	$0.3 \times 10^{-13}$
16	$1.4 \times 10^{-13}$	$0.4 \times 10^{-13}$	$1.7 \times 10^{-13}$	$0.6 \times 10^{-13}$
32	$1.4 \times 10^{-13}$	$0.5 \times 10^{-13}$	$1.5 \times 10^{-13}$	$0.9 \times 10^{-13}$

TABLE VII (continued)  
COMBINED ADEV BETWEEN OQ291 AND OQ315 OSCILLATORS

$\tau$ (s)	A7 ADEV	A7 Uncertainty	5110A ADEV	5110A Uncertainty
1	$1.6 \times 10^{-13}$	$0.05 \times 10^{-13}$	$1.9 \times 10^{-13}$	$0.01 \times 10^{-13}$
2	$1.6 \times 10^{-13}$	$0.06 \times 10^{-13}$	$1.5 \times 10^{-13}$	$0.01 \times 10^{-13}$
4	$1.7 \times 10^{-13}$	$0.09 \times 10^{-13}$	$1.5 \times 10^{-13}$	$0.01 \times 10^{-13}$
8	$1.9 \times 10^{-13}$	$0.1 \times 10^{-13}$	$1.6 \times 10^{-13}$	$0.02 \times 10^{-13}$
16	$2.1 \times 10^{-13}$	$0.2 \times 10^{-13}$	$1.7 \times 10^{-13}$	$0.03 \times 10^{-13}$
32	$2.1 \times 10^{-13}$	$0.3 \times 10^{-13}$	$1.9 \times 10^{-13}$	$0.04 \times 10^{-13}$

The IREE-DMTD and IEN-DMTD systems have shown the combined values of  $ADEV(\tau=1s) = 1.4 \times 10^{-13}$  and  $1.3 \times 10^{-13}$ , respectively, which are consistent with the uncertainty. Since  $\Delta x$  was adjusted within the optimum interval during the measurement, the noise contribution of the measurement systems is only about 4 %. Considering the corrected combined value to be  $1.3 \times 10^{-13}$  then by dividing this amount by  $\sqrt{2}$  we obtain a slightly poorer stability than that specified for each individual oscillator in Fig.6 where, however, no uncertainties are given. The A7 and 5110A systems show combined values of  $ADEV(\tau=1s) = 1.9 \times 10^{-13}$  and  $1.6 \times 10^{-13}$ , respectively, from which their noise contribution can be calculated. It gives approximately  $9 \times 10^{-14}$  for A7 and  $1.3 \times 10^{-13}$  for 5110A. Since in the case of A7 and 5110A

no specification of  $\Delta x$  is given, it was set randomly. Thus actually the noise floors may assume any value shown in Table III and Table IV, respectively.

The stability between the uncorrelated 5 MHz test signals was also evaluated in the frequency domain. The result in terms of common  $L(f)$ , single-sideband phase noise to carrier power, is shown in Fig. 12.

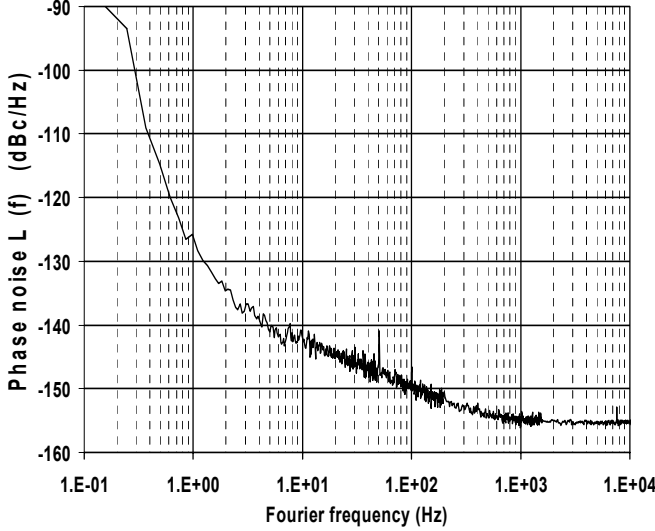


Fig. 12. Phase noise between uncorrelated test signals.

The value of  $L(f)$  is about -128 dBc/Hz at  $f=1$ Hz which, by making conversion to the time domain for flicker-frequency noise, corresponds to  $ADEV=1.3 \times 10^{-13}$ .

#### RF POWER DEPENDENCE

In an ideal measurement setup the results must be insensitive to the boundary conditions. Obviously, in a real setup this is not true. When we make use of sensitivity-enhancement techniques with phase-difference multiplication by large factors we can observe effects which were previously too small to be noticed. Improving resolution by over three orders of magnitude will expose effects previously unobserved. In this paragraph we will shortly examine the behavior of the DMTD systems under changes of input signal levels.

In seeking the best measurement capability of each measurement system we have experimented a significant impact on Allan variance and on counter time-interval readings with the level of signals. This can be explained by the change in beat signal slope with input power. If mixers work within linear conditions (with power at the RF input lower than that at the LO input) the voltage amplitude of the sine-wave beat signal is

$$V_0 = \sqrt{R_0 P_{rf} I_m} \quad (1)$$

where  $R_0$  is the load resistance at the IF mixer output port,  $I_m$  ( $I_m < 1$ ) is the mixer loss and  $P_{rf}$  is the power at input RF mixer port. The beat signal slope around the zero-crossing is  $s = 2\pi \Delta v \cdot V_0$ . In the presence of noise the beat signal crosses the zero with an rms time jitter  $\sigma_x = \sigma_n / s$ , where  $\sigma_n$  is the total rms voltage noise amplitude in the bandwidth of interest. The corresponding phase fluctuation spectral density  $S_\phi(f) = 4\pi^2 S_x(f)$  and relative frequency fluctuation spectral density  $S_y(f) = (f/v_0)^2 S_\phi(f)$  are thus:

$$S_\phi(f) = \frac{1}{\Delta v^2 R_0 P_{rf} I_m} S_n(f) \quad (2)$$

$$S_y(f) = \frac{1}{v_0^2 \Delta v^2 R_0 P_{rf} I_m} S_n(f) \cdot f^2 \quad (3)$$

where  $f$  is the Fourier frequency,  $v_0$  is the carrier frequency,  $S_x(f)$  is the time deviation spectral density and  $S_n(f)$  is the voltage noise spectral density. From the relationship between spectral densities and the Allan variance ( $AVAR = ADEV^2$ ) we can write

$$AVAR(\tau) = \frac{3}{4\pi^2} \cdot f_h \cdot \frac{S_{n,w}}{v_0^2 \Delta v^2 R_0 P_{rf} I_m} \cdot \tau^{-2} \quad (4)$$

for white voltage noise with  $S_n(f) = S_{n,w}$  and

$$AVAR(\tau) = \frac{3}{4\pi^2} \cdot \ln(2\pi f_h \tau) \cdot \frac{S_{n,f}}{v_0^2 \Delta v^2 R_0 P_{rf} I_m} \cdot \tau^{-2} \quad (5)$$

for flicker voltage noise with  $S_n(f) = S_{n,f} / f$ , where  $f_h$  is the upper cutoff frequency and  $S_{n,f}$  is the spectral density value at the Fourier frequency of 1 Hz.

From these expressions we have estimated the noise floor expected for the IEN design [6]. With regard to each ZCD the estimated white and flicker-noise voltage densities are  $S_{n,w} \approx 4 \text{ nV}^2/\text{Hz}$  and  $S_{n,f} \approx 4 \text{ nV}^2$ , respectively, with a predominant contribution from the first linear stage. With a 5 mW (+7 dBm) RF signal power and considering the upper cutoff frequency  $f_h$  equal to the equivalent noise bandwidth of the first stage, we obtain  $ADEV(\tau) \approx 6 \times 10^{-15}/\tau$  and  $ADEV(\tau) \approx 3 \times 10^{-15}/\tau$  for white and flicker contribution.

A further consistent contribution comes from the mixer flicker noise. It has been estimated by means of the frequency-domain noise-floor of  $S_\phi(1 \text{ Hz}) \approx 5 \times 10^{-15} \text{ rad}^2/\text{Hz}$  measured in a phase-noise measurement setup (with the mixer used in the DMTD system) for a 5 MHz carrier frequency with 5 mW power level. For this noise contribution an expected value of  $ADEV(\tau) \approx 8 \times 10^{-15}/\tau$  can be derived.

From this computation we expect a noise floor for the DMTD system of  $ADEV(\tau) \approx 1.5 \times 10^{-14}/\tau$ , including these three noise contributions, for two independent channels. This value does not account for common oscillator noise contribution [11, 12].



In a similar way we could explain the variations in counter time-interval reading with the signal level taking into account small offset voltage in ZCDs and DC voltage at the IF mixer output due to slight mismatch in the diode bridge and imperfect balance in the transformer windings. Consider again a sine-wave beat signal with a slope  $s$  close to the zero crossing with an offset voltage  $v_{\text{off}}$  at the ZCD input. The consequence of the offset appears to be a time bias  $\delta t = v_{\text{off}} / s$  with respect to the ideal zero-crossing time instant. The resulting bias in time-interval measurement depends on the ratio between the voltage offset and voltage amplitude of the beat note. A rough test of the IEN-DMTD system sensitivity versus common oscillator power is reported on Fig. 13. This graph reports the mean counter readings (divided by multiplication factor) at several values of common oscillator output power. For this measurement we have used the HP 8662 frequency synthesizer instead of the Milliren quartz oscillator. The straight line interpolation gives a 15 ps/dBm mean value for the power sensitivity of this system.

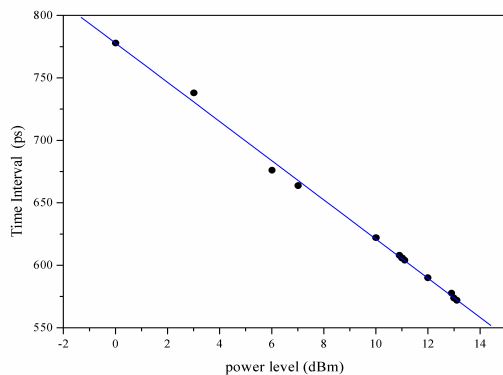


Fig. 13. Time interval vs. common oscillator power.

## CONCLUSIONS

Considering the background noise in terms of ADEV( $\tau=1s$ ) as the main criterion for assessment of the system performance, the IREE-DMTD and IEN-DMTD laboratory systems have shown better than the commercial ones. Still in assessing the performance of the compared systems one should take into account also the purpose of each of them. Thus the IREE-DMTD and IEN-DMTD systems are transparent structures which, besides being employed in practical measurements, are primarily used as the subject of study. Therefore we treated them appropriately and we knew what we could expect from them. In contrast, the commercial systems A7 and 5110A are intended as practical tools in time/frequency measurements. Thus they should be compact and user-friendly, and all needed information should be provided in the manual. It was not so, specially in the case of the A7 system. For instance there was no information on the strong dependence of the noise floor on the input phase difference. In fact we do not under-

stand this effect in this type of frequency-difference multiplier. In a variety of measurements that we have carried out with the four systems, the 5110A unit showed, thanks to appropriate signal and data manipulation, the most practical one and by far most user-friendly. It should be pointed out, for instance, that with maximum relative frequency deviation of  $1 \times 10^{-8}$  between the test signals, the 5110A still provided the same results within the measurement uncertainty as in the near-equal-frequency case. The great advantage of the 5110A analyzer over other tested systems is also much faster sampling rate ( $\tau = 10$  ms). This allows averaging that can be helpful in short-term phase-stability analysis.

## ACKNOWLEDGMENT

The authors thank Prof. Juan Palacio of ROA and Mr. Petr Zacharias of MLCAF for their contribution to the successful realization of the measurements.

## REFERENCES

- [1] L.S. Cutler and C.L. Searle, "Some aspects of the theory and measurement of frequency fluctuations in frequency standards," *Proc. IEEE*, 54(2), 136-154, 1966.
- [2] D.W. Allan and H. Daams, "Picosecond time difference measurement system," *Proc. 29<sup>th</sup> Annu. Symp. Frequency Contr.*, Atlantic City, NJ, pp. 404-411, May 1975.
- [3] S.R. Stein, in *Precision Frequency Control*, vol. II, E.A. Gerber and A. Ballato, Eds. New York: Academic Press, 1985, pp. 229-231.
- [4] V.F. Kroupa, *Frequency Synthesis*, London, Griffin, 1973, pp. 242-243.
- [5] R. Barillet, "Comparateur de phase ultra faible bruit pour les futurs étalons de fréquence," *Proc. European Forum on Time and Frequency*, Besancon (France), pp. 249-254, March 1989.
- [6] G. Brida, "High resolution frequency stability measurement," *Rev. Sci. Instrum.*, vol. 73, No. 5, pp. 2171-2174, May 2002.
- [7] "TSC 5110A time interval analyzer," User Manual, Timing Solution Corporation, April 2001.
- [8] D. Fredlake, Timing Solutions Corporation, Private communication, April 2003.
- [9] "Model A7 frequency and phase comparator," *Users Handbook*, Quartzlock Instruments, July 1998.
- [10] "Stable32 version 1.35: frequency stability analysis," Hamilton Technical Services, S. Hamilton, MA 01982 USA, 2002.
- [11] C.A. Greenhall, "Common-source phase noise of a dual-mixer stability analyzer," TMO Progress Report 42-143, Jet Propulsion Laboratory, Pasadena, XA, November 2001.
- [12] L. Sze-Ming, "Influence of Noise of Common Oscillator in Dual-Mixer Time-Difference Measurement System," *IEEE Trans. on Instr. and Meas.*, Vol. IM-35, No. 4, December 1986, pp. 648-651.